

## VISION BASED TRACKING CONTROLLER FOR AN ON-ORBIT METEOR OBSERVER

Ravi teja Nallapu,<sup>\*</sup> Aaditya Ravindran,<sup>†</sup> and Jekanthan Thangavelautham<sup>‡</sup>

The Earth faces potential danger from Meteors that enter its atmosphere. During their entry, these objects begin ablating due to atmospheric friction and often exploding in the atmosphere. Consequently, large amount of energy is released during this airburst. The Chelyabinsk meteor event of 2013 is an iconic example of the potential danger, where the airburst released about 500 kilotons of energy. This motivates the need for a timely surveillance system which can help us better prepare for such dangers. The Space-based Wide-angle Impact of Meteors Satellite (SWIMSat) is a CubeSat mission being built by the University of Arizona to monitor the Earth for meteoric entry events. SWIMSat uses a body fixed, wide field of view visible camera to look for meteor impacts. When an entry event is observed, SWIMSat will detect this event by optically detecting the trail of the entering meteor, and then track the trajectory of the meteor in the image plane by using its attitude control system. The objective of this paper is to present the implementation of the vision-based tracking system for the SWIMSat mission. A color based (hue, saturation, and value) detection and tracking method is presented to observe and track the meteors entering the atmosphere. The detection is achieved by calibrating the algorithm to isolate only those pixels which have a color range of a typical entry event. The algorithm then finds the center of the event, by fitting the maximum bounding rectangle around the isolated pixels. A tracking error is then calculated based on the center of the detected event, and the center of the camera. The error is then converted into an attitude command which is sent to the attitude control system to regulate the tracking error. This results in the camera centering on the target event. A hardware demonstration of the algorithm is also presented here. The algorithm is demonstrated by using equivalent low-cost equipment in place of the actual flight hardware. The developed testbed consists of a standard webcam to simulate the imaging system of SWIMSat, and a robotic arm to simulate the spacecraft attitude control system. The algorithm is run on a laptop, which acts as the spacecraft computer. The entry event is simulated by displaying a simulation of Earth entering meteors. The algorithm is calibrated to isolate events in the color range of the simulated meteor. A PID control law, based on the generated tracking error, is developed for the robotic arm to maneuver the camera and align the cam-

---

<sup>\*</sup> Graduate student, Department of Aerospace and Mechanical Engineering, University of Arizona.

<sup>†</sup> Graduate student, School of Electrical, Computer and Energy Engineering, Arizona State University.

<sup>‡</sup> Assistant Professor, Department of Aerospace and Mechanical Engineering, University of Arizona.

era center with the center of the detected event. The results of the demonstration show that the controller can achieve stable tracking within 3 seconds. These results show promise that such a tracking system can indeed enable SWIMSat to detect and track meteor entry events.

## INTRODUCTION

On February 15, 2013, a 17 m meteor entered the Earth's atmosphere near Chelyabinsk, Russia culminating in a violent airburst that released 500 kilotons of energy. Fortunately, the airburst occurred at 30 km altitude<sup>1</sup>, causing no casualties, but several injuries and much property damage was incurred at the site. These events are not too rare and are expected once every 50 years. Between 1988-2018, US government sensors recorded at least 604 meteor events of various energies ranging from 0.1 Kiloton to the 500 kilotons all around the world<sup>2</sup>.



**Figure 1. The entry of the Chelyabinsk meteor observed from the ground just before its airburst.**

Meteoritic impacts, such as the Chelyabinsk, are a classic example of the dangers posed by atmospheric entry events. Objects of about 1-50 m diameter may be impacting an order of magnitude more frequently than usual, perhaps due to recent breakups or other dynamical events. Particularly, objects of diameter 10 m and larger, upon atmospheric entry can cause explosions leading to a release of few hundreds of kilotons of energy<sup>3</sup>. Similar risks also exist from man-made objects such as long-range missiles and reentering space debris<sup>4</sup>.

A problem that is common to all these reentry events is that, most of these events are recorded after their impact, which is often too late. This mandates the need for having a space-based monitoring network which can provide early warning when a dangerous meteor entry event occurs.

The SWIMSat<sup>3,7</sup> mission being built by the University of Arizona, aims to make the first step towards building such a network of Earth monitoring spacecrafts for improving the space situational awareness (SSA) of meteor entry events. SWIMSat is a 3U CubeSat, which will be deployed in Low Earth Orbit (LEO) with an optical camera as its payload. SWIMSat's mission is to perform long-term, dedicated observations of Earth. The onboard spacecraft computer continuously runs an event detection algorithm on the lookout for fire trails of ablating meteorites. Once an event is

detected, the algorithm estimates a tracking error based on the difference in centers of the entry event and the camera in the image plane. The tracking error is used by the onboard computer to generate an attitude correction command which is then sent to the onboard reaction wheels.

The objective of this paper is to present the implementation of the vision-based tracking algorithm for the SWIMSat spacecraft. Hardware-in-the-loop testing of the algorithm is carried out, and the results of the testing show promise that such a system can indeed be deployed on SWIM-Sat for its meteor observing mission. The paper proceeds by first presenting a brief overview of the SWIMSat mission, where the concept of operations and major subsystems are described. Following this, the algorithm for the vision-based tracking system is described. Then a detailed description of the hardware testing of the algorithm is provided, followed by the results of this demonstration. Finally, a summary of the work is provided along with a discussion of the achievements and future direction for the vision based tracking software onboard the SWIMSat spacecraft.

## SWIMSAT MISSION

As mentioned above, the Space-based Wide-angle Imaging of Meteors Satellite (SWIMSat) is 3U CubeSat to observe meteors during their atmospheric entry<sup>3,7</sup>. Once an entry event is observed, it is detected by isolating the fiery trail being lit. This event is then tracked till the entry phase of the meteor is completed, after which the meteor trail is extinguished. Once no event is detected the spacecraft reenters its observing mode. The concept of operation of the SWIMSat mission is presented in Figure 2.

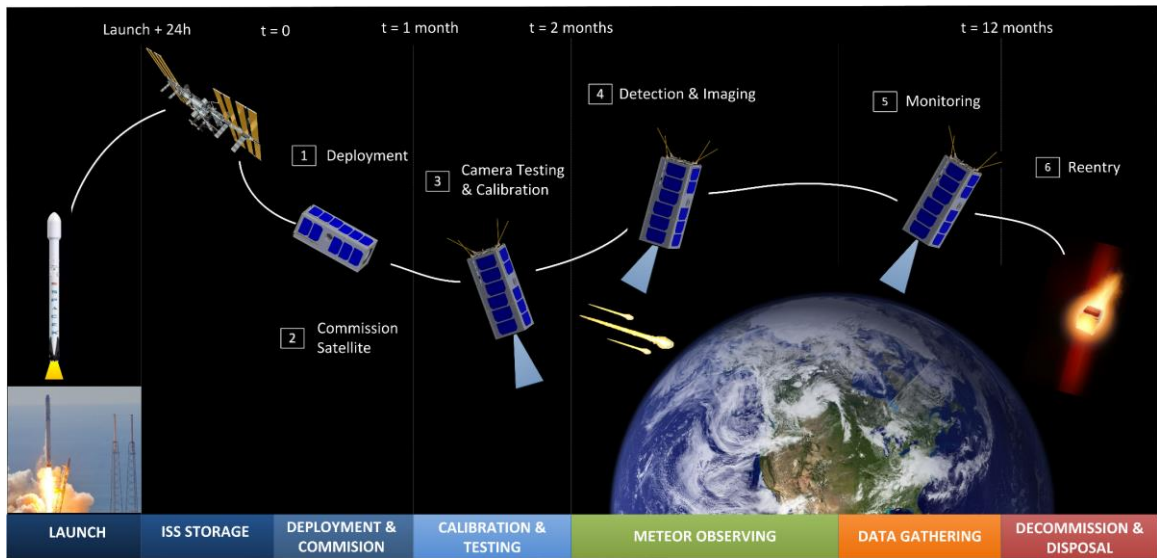


**Figure 2. Concept of operation for the SWIMSat mission**

As seen in Figure 2, once the spacecraft is commissioned and calibrated, the spacecraft begins its meteor observing phase, where the camera uses its body fixed camera to point to the center of Earth. SWIMSat uses a CMOS camera PHY367C coupled with a wide-angle field of view lens: Tech Spec C, which provides a field of view of 143 Deg. Once an entry event is observed, the onboard algorithm will detect the event by a color detection thresholding and centroiding algorithms, which compute an attitude error: the difference between the center of the observed event, and center of the camera. The algorithm runs on the onboard command and data handling

(CD&H) subsystem. SWIMSat has selected the CSP C&DH board by Space Micro. A proper functioning of the algorithm also requires a calibration of the camera to establish the thresholding limits, which will be presented in the next section.

The error is then regulated by the onboard attitude control system. SWIMSat uses MAI-400 by Maryland Aerospace Inc, for its attitude determination and control system (ADCS). The ADCS has 3-axis reaction wheels, and 3-axis magnetorquers, along with an attitude determination suite to maneuver the spacecraft towards the desired attitude. The process is repeated until the entry event is finished. After the data is gathered by the spacecraft, SWIMSat will downlink the data using a UHF radio system. The radio communication system consists of the AstroDev Litium-1 radio and a Nanocom ANT 430 antenna. A sectional view of the SWIMSat spacecraft along with its different subsystems is presented in Figure 3.

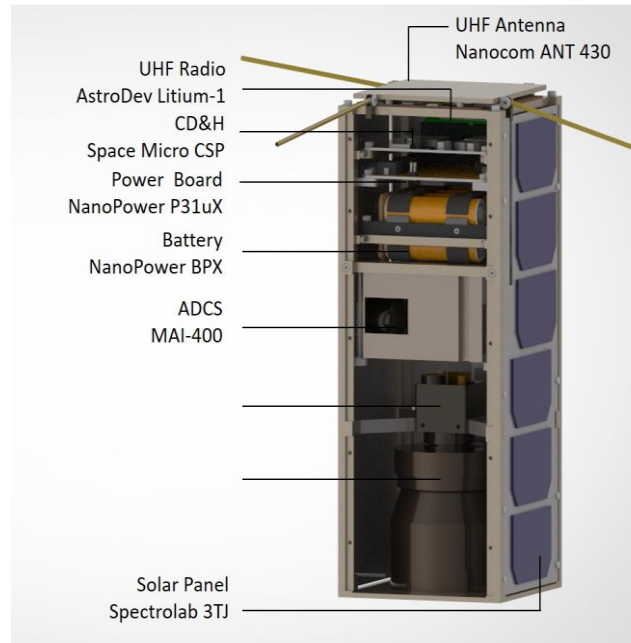


**Figure 3. Sectional view of the SWIMSat spacecraft to present various subsystems**

## THE ALGORITHM

The vision-based detection algorithm works by using observing events within a certain color range. The color of an object is described by a 3 parameter cylindrical coordinates: hue-saturation-values (HSV)<sup>5</sup>. Therefore, detecting an event in this system can be accomplished by observing objects only in a defined range of hue-saturation value coordinates as presented in Equation 1:

$$(h_{min}, s_{min}, v_{min}) \leq (h, s, v) \leq (h_{max}, s_{max}, v_{max}) \quad (1)$$

The values of minimum and maximum coordinates in Equation 1 are determined during calibration, where the spacecraft captures images of known entry event without detecting them. These images are downlinked, to the ground station where they are processed to determine the bounds. The bounds are then uplinked to the SWIMSat, where it is now ready to begin its observing

phase. Therefore, in the observing phase, the SWIMSat computer will isolate only those pixels which fall in the thresholded range, as shown in Figure 4.

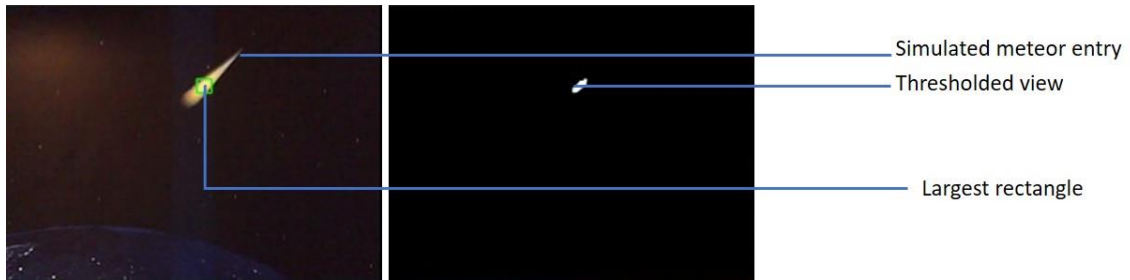


**Figure 4. Camera view of SWIMSat is shown on the left, and the corresponding thresholded image shown on the right. Once thresholded, the algorithm draws the largest rectangle around the pixels.**

In the second part of the algorithm, those image frames flagged to contain meteor events is automatically stored. During this phase, the event is tagged by drawing a bounding rectangle around the largest set of pixels that span the thresholded view as shown in Figure 4. This is accomplished by extracting color contours in the thresholded view and then fitting the maximum bounding rectangle around these contours<sup>6</sup>. The location of the center of this event rectangle, in the image space relative to the center of the image, is used to correct the attitude of the spacecraft. The geometry of the meteor detection in a 2-dimensional image space is presented in Figure 5. The position error of the event with respect to the center of the camera can be given by Equation 2 as:

$$(x_{err}, y_{err}) = (x_e - x_c, y_e - y_c) \quad (2)$$

Where the subscripts err, e and c denote the coordinates for error, event and camera respectively.

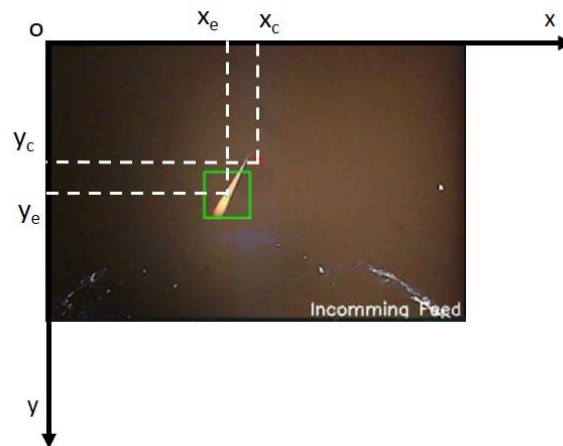


**Figure 5. Image frame coordinate system to show the coordinates of the center of the image and center of the detected event.**

The position errors generated in Equation 2 are used to generate reference commands for the ADCS subsystem to align the camera center with the center of the event. Figure 6 provides a summary of the vision-based tracking algorithm.

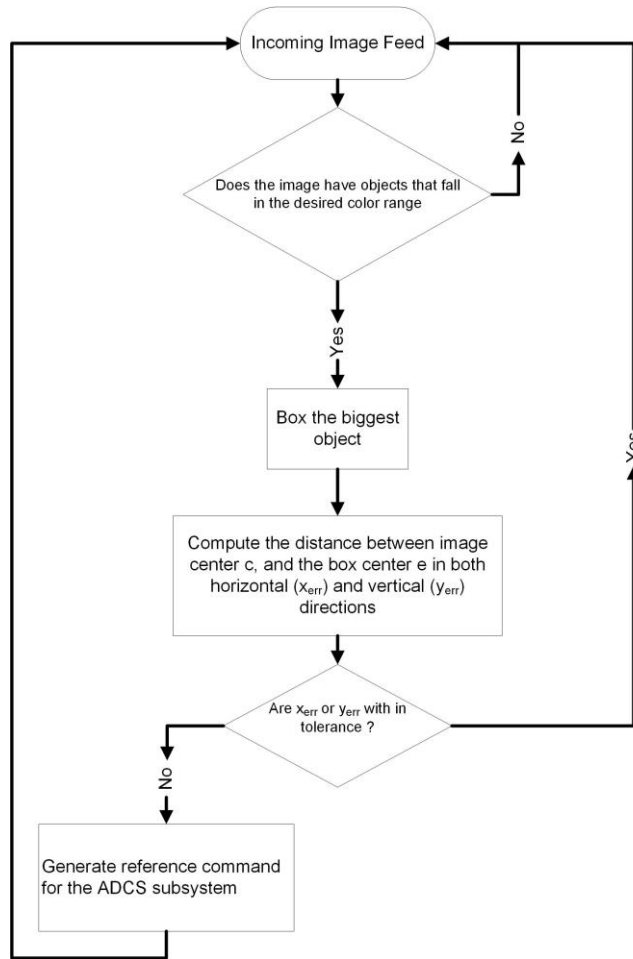


**Figure 6. Algorithm for the vision-based tracking controller of SWIMSat**

## TESTING

To demonstrate the performance of the algorithm, a testbed was constructed to simulate meteor entry. The spacecraft in this setup is simulated by a computer webcam. The camera is mounted on a robotic arm setup which can move in the image space shown in Figure 5. The robotic arm is used as a simulator for the ADCS subsystem. The robotic arm and the camera are connected to control computer which simulates the C&DH subsystem.

A graphical simulation of meteors entering the Earth’s atmosphere was developed using the 3D vector graphics module of MATLAB. These simulations are placed in the field of view of the camera as shown in Figure 7. After calibrating the images, the tracking of the meteors was demonstrated. The trajectory of the simulated meteor entry is recorded for different simulations and is presented in the results.

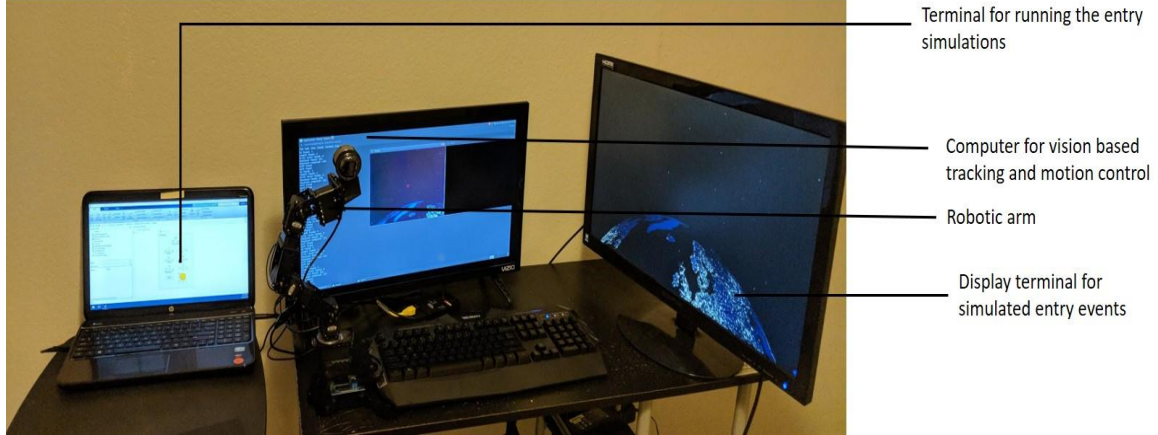


**Figure 7. Setup of the algorithm demonstration testbed**

*Controller design.* As mentioned above, the ADCS of SWIMSat was simulated by a robotic arm, which has 2 degrees of freedom: a pan angle ( $\theta$ ) and a tilt angle ( $\phi$ ) along the camera  $x$  and  $y$ -axis respectively. A PID control law is developed by using the position error feedback from the camera to track the meteor event simulation. The implemented control law for the pan and tilt angles are shown in Equations 3 and 4 respectively. Where the  $K_p$ ,  $K_i$ , and  $K_d$  represent the proportional, integral, and derivative gains respectively. Due to the similarity of all the degrees of freedom on the robotic arm equal gains were used for both the pan and tilt motion as captured by Equations (3) and (4). These angles are then sent to the robotic arm system to align the camera center with the center of the detected event.

$$\theta = -K_p x_{err} - K_i \int_0^t x_{err} dt - K_d \dot{x}_{err} \quad (3)$$

$$\phi = -K_p y_{err} - K_i \int_0^t y_{err} dt - K_d \dot{y}_{err} \quad (4)$$

*Demonstration.* The performance of the vision tracking algorithm was demonstrated on the testbed described above. The HSV bounds described in Equation 1 were found by calibrating the camera to detect the spectrum of the simulated meteors. Then the control gains in Equations 3 and 4 were found by adjusting the gains to obtain a smooth response. Table 1 presents the parameters used during the demonstration.

**Table 1. Parameters used for the algorithm demonstration.**

Parameter	Description
$(h_{min}, s_{min}, v_{min})$	(0, 0, 254)
$(h_{max}, s_{max}, v_{max})$	(172, 14, 255)
$K_p$	4
$K_i$	0.05
$K_d$	0.5

The algorithm is demonstrated for 2 cases: when the object detected is stationary, and when the object detected is moving. In both cases, the position of the detected event relative to the center of the camera is recorded dynamically. The recorded results are presented in the next section.

## RESULTS

As described in the previous section, two simulations were run: to demonstrate stationary and motion tracking. The error coordinates that specify the relative position of the event with respect to the image center are given by Equation 2, along with the magnitude of the error ( $E$ ) given by Equation 5 as

$$E = \sqrt{x_{err}^2 + y_{err}^2} \quad (5)$$

*Stationary object tracking.* In the first simulation, the meteor is held fixed on the display, and the robotic arm, based on the feedback from the camera, tries to align the center of the camera to the fixed location. The result of this tracking is shown in Figure 8.

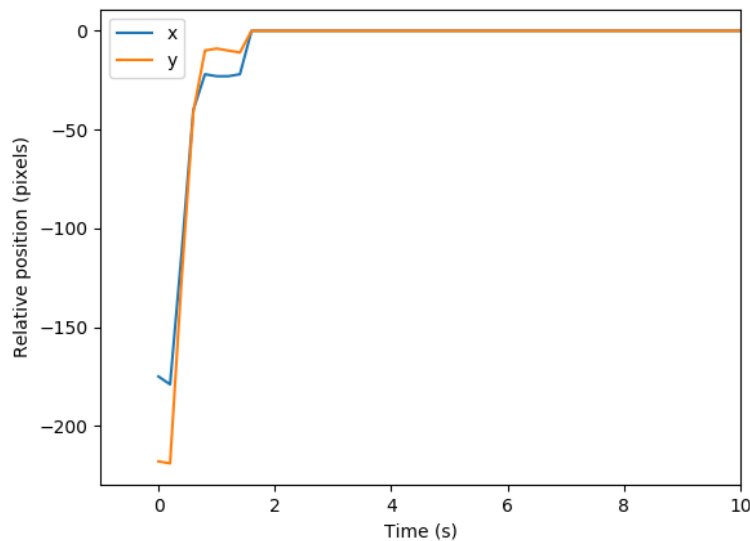


**Figure 8. The relative position of the center of the detected event with respect to the camera center during the stationary event detection. Center of the camera converges to the center of the detected event in 1.6 seconds**

As seen here in Figure 8, the event starts at a different location than the screen center, and the controller aligns the two centers. A stable centering was achieved in about 2 seconds during which the tracking error was reduced below 1 pixel as shown in Figure 9.



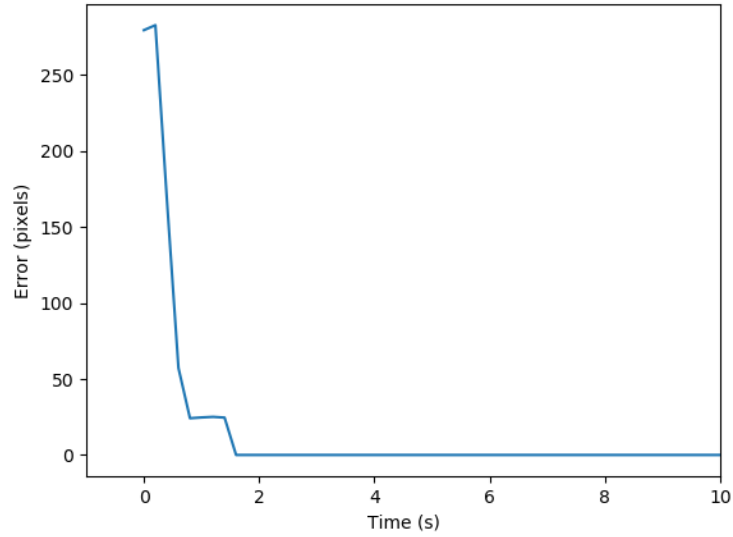


**Figure 9. The magnitude of the tracking error. The tracking error is reduced in 1.6 seconds.**

*Moving object tracking.* In the second simulation, the meteors appear randomly and move on the display monitor, while the robotic arm tries to align the center of the camera to the moving object. The results of this tracking are shown in Figure 10.

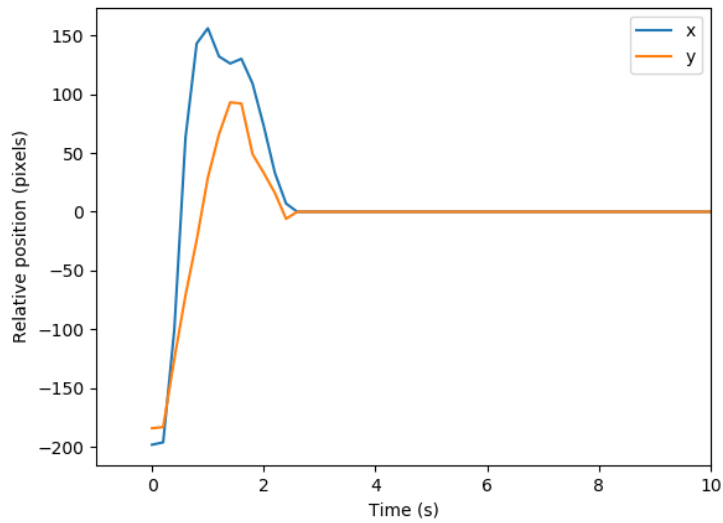


**Figure 10. The relative position of the center of the detected event relative to the camera center in the moving event detection. A slight overshoot was observed, and the centers were aligned in 2.6 seconds.**

As seen here in Figure 10, once the event was detected, the controller aligned the center of the camera with the center of the event within 3 seconds. The stable centering with a tracking error less than 1 pixel was achieved during this time, as shown in Figure 11.

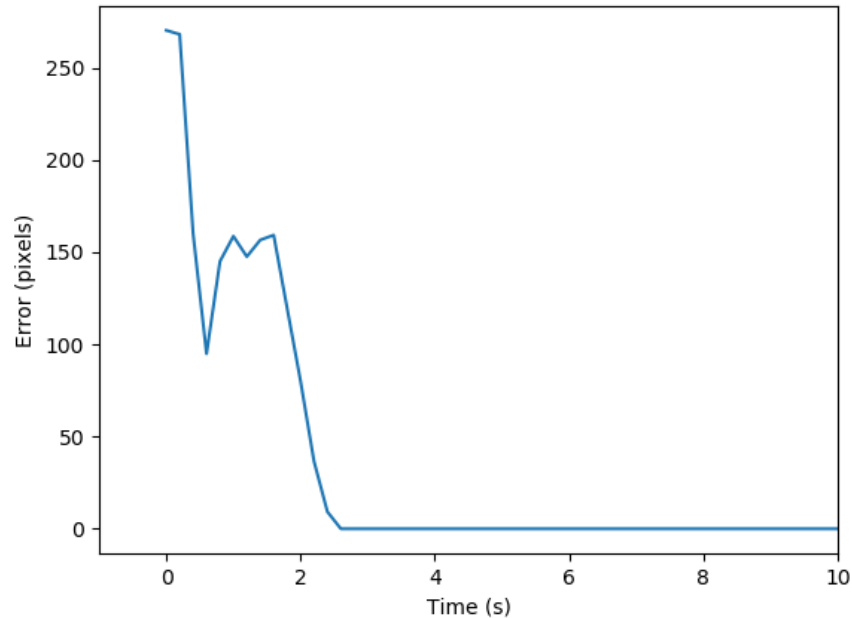


**Figure 11. The magnitude of the tracking error. The controller settles down to a stability of about 20 pixels in 3 seconds.**

## CONCLUSION

In this work, we presented a vision-based tracking system that was developed for tracking objects from space. The tracking method developed will be used by SWIMSat (Space-based Wide-angle Imaging of Meteors Satellite) which is a Low Earth orbit (LEO) based 3U CubeSat. The SWIMSat mission uses a wide field of view imaging system to observe the Earth during the nighttime for atmospheric entry events. The camera is placed on the long axis of the spacecraft so that the earth observation is achieved with Nadir pointing. While monitoring the Earth, the SWIMSat uses an onboard image processing to detect meteors by isolating the pixels of the fiery trail of a meteor on its entry. Once detected, SWIMSat uses its onboard reaction wheels to point itself towards the direction of the entering meteor and track its trajectory. The performance of the tracking system was demonstrated by constructing a testbed with standard parts such as a webcam, laptop, and a robotic arm. The webcam simulates the payload of the SWIMSat, spacecraft while the robotic arm simulates its attitude control system. The image processing is done on the laptop which acts as the onboard computer. The entry of meteors was simulated by a computer-based simulation. Once the event is detected by the camera, the robotic arm tries to keep the camera focused on the trajectory of the event being observed by employing a PID control law to track the meteor.

The results suggest a successful demonstration of the tracking algorithm, where the controller was able to achieve a stable tracking within 3 seconds, with a tracking error of less than 1 pixel. The results show promise that such a tracking system can indeed enable SWIMSat to detect and track reentry events. The results of this work demonstrate achieving the minimum requirements for SWIMSat. However, efforts are being made to improve the functionality of the algorithm. Having implemented a simple tracking system, the algorithm can be improved by capturing the dynamics of the reentry process of a meteor. The algorithm can also be advanced to detect the signatures of the entry event to provide further compositional insight into the entering object.

## REFERENCES

- <sup>1</sup> Popova, O. P., et al. "Chelyabinsk Airburst, Damage Assessment, Meteorite Recovery, and Characterization." *Science*, 342 (6162), 2013. Post-Print Version, vol. 342, no. 6162, 2013, pp. 1069-1073.
- <sup>2</sup> "Fireball and Bolide Data." *NASA*, NASA, [cneos.jpl.nasa.gov/fireballs/](http://cneos.jpl.nasa.gov/fireballs/).
- <sup>3</sup> Hernandez, V., Gankidi, P., Chandra, A., Miller, A., Scowen, P., Barnaby, H., Adamson, E., Asphaug, E., Thangavelautham, J., 8220; SWIMSat: Space Weather and Meteor Impact Monitoring using a Low-Cost 6U CubeSat," Proceedings of the 30th Annual AIAA/USU Conference on Small Satellites, AIAA, Logan, Utah, 2016.
- <sup>4</sup> Hankey, Wilbur L., and Inc ebrary. Re-Entry Aerodynamics. American Institute of Aeronautics and Astronautics, Washington, D.C, 1988, doi:10.2514/4.862342.
- <sup>5</sup> Zetterlind III, Virgil E., and Stephen M. Matechik. Hue-Saturation-Value Feature Analysis for Robust Ground Moving Target Tracking in Color Aerial Video, vol. 6235, SPIE, 2006, doi:10.1117/12.666728.
- <sup>6</sup> Suzuki, Satoshi, and Keiichi Abe. "Topological Structural Analysis of Digitized Binary Images by Border Following." *Computer Vision, Graphics and Image Processing*, vol. 30, no. 1, 1985, pp. 32-46.
- <sup>7</sup> Hernandez, V., Ravindran, A., Herreras-Martinez, M., Asphaug, E., Thangavelautham, J., "On-Orbit Demonstration of the Space Weather and Meteor Impact Monitoring Network," Proceedings of the 31st AIAA/USU Small Satellite Conference, 2017.